The instability of liquid surfaces when accelerated in a direction perpendicular to their planes. II

By D. J. Lewis, *Engineering Laboratory, University of Cambridge*

(*Communicated by Sir Geoffrey Taylor, F.R.S.—Received* 3 *December* 1949)

[Plates 5 to 11]

An apparatus for accelerating small quantities of various liquids vertically downwards at accelerations of the order of $50g$ (g being 32·2 ft./sec.^{2}) is described, and the behaviour of small wave-like corrugations initially imposed on the upper liquid surface has been observed by means of high-speed shadow photography. The instability observed under a wide variety of experimental conditions has been analyzed, and the initial phases have been found to agree well with the first-order theory given in part I.

When the disturbance has attained a considerable amplitude the first-order equations cease to apply and it changes from a wave into a form which has the appearance of large round-ended columns of air extending into the liquid and separated by narrow sheets of liquid. The air columns attain a steady velocity relative to the accelerating liquid and continue to penetrate into the liquid until the lower surface of the liquid is reached.

In spite of these very large surface disturbances, the main body of liquid below them is accelerated as though they did not exist.

1. Introduction

The experiments described in this paper were designed to test the validity of Sir Geoffrey Taylor's first-order theory (given in part I, Taylor 1950) for the instability of an initially disturbed sheet of liquid when subsequently accelerated. It is shown in part I that the increase in amplitude of a two-dimensional disturbance accelerated downwards at an acceleration g_1 is given by

$$\frac{\eta}{\eta_0} = \cosh \sqrt{\left\{\frac{4\pi s}{\lambda}\frac{(g_1-g)}{g_1}\frac{(\rho_2-\rho_1)}{(\rho_1+\rho_2)}\right\}}, \tag{1}$$

where η, η_0, s, λ, ρ_1, ρ_2, g_1 and g are as defined in part I.

The experimental apparatus was so constructed that a range of accelerations of from $3{\cdot}0g$ to $140g$ (g being 32·2 ft./sec.^{2}) could be applied to various depths of liquid of from $\frac{3}{8}$ to 20 in.

2. Description of apparatus and its operation

A photograph of the acceleration apparatus is given as figure 1. The liquid is initially supported in a vertical channel whose cross-section is $2\frac{1}{2} \times \frac{1}{2}$ in. by means of a thin brittle diaphragm inserted between the flanges A joining together the two glass-sided observations ducts B and C. After many trials with glass, waxes, paper, etc., a technique was developed for making diaphragms which would break at a pressure equivalent to as little as 2 in. of water and yet would not leak under a steady pressure equivalent to 1 in. of water. These diaphragms were made of shellac of thickness 0·001 to 0·007 in.

The portion of the apparatus above the liquid is airtight and that below the liquid is also rendered airtight when a glass disk is clamped between the flanges D at the bottom of the apparatus. Air is then admitted through the pipes E and F from a single source of compressed air, so that the pressure of the air above the liquid is raised at the same rate as the pressure of the air below the liquid.

When the desired pressure has been reached, the volumes of air above and below the liquid are isolated from each other and from the compressed air supply. At the

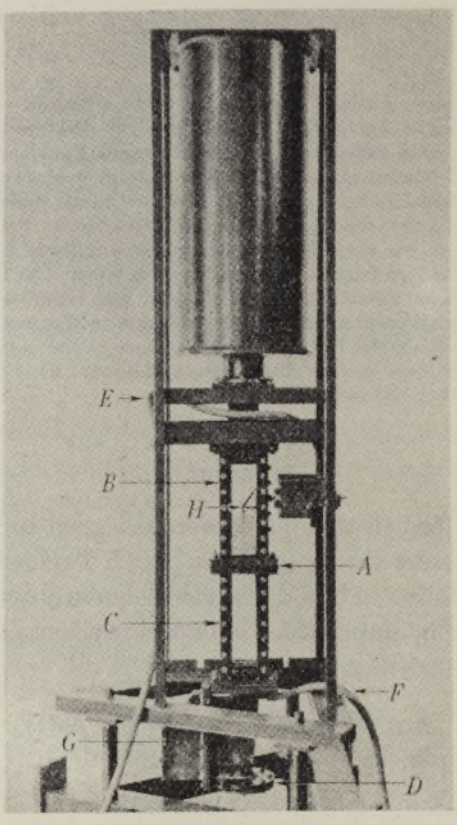

FIGURE 1. The acceleration apparatus.

appropriate instant, a mechanism inside the cover G is released electrically which breaks the glass disk held between the flanges D. The resulting rarefaction wave travels up the apparatus, and the shellac diaphragm breaks completely and allows the liquid to accelerate downwards under the action of the compressed air above it.

By this technique, a column of liquid of height 9 in. can be accelerated at accelerations of up to $75g$ and smaller columns of liquid at proportionately higher accelerations. The top surface of the liquid can be given an initial surface disturbance by means of the agitating paddle H which is actuated by a motor and mechanism in the box seen to the right of the observation duct B.

The downward motion of the liquid is recorded by means of shadow photography through the two pairs of toughened glass windows B and C. The arrangement of the

photographic apparatus is shown in figure 2. The illumination is provided by discharges of charged condensers across four spark gaps which are arranged in two groups. Two spark gaps separated by a thin sheet of mica are placed on the optical axis of a condensing lens J which concentrates their light flashes into the lens of a quarter-plate camera K fitted with a $f/8$ lens of 6 in. focal length. The effective area of the condensing lens is increased by the use of a spherical mirror L which produces an image of the spark gaps a few inches in front of their actual position. By this means a 7 in. length of the upper window B is illuminated.

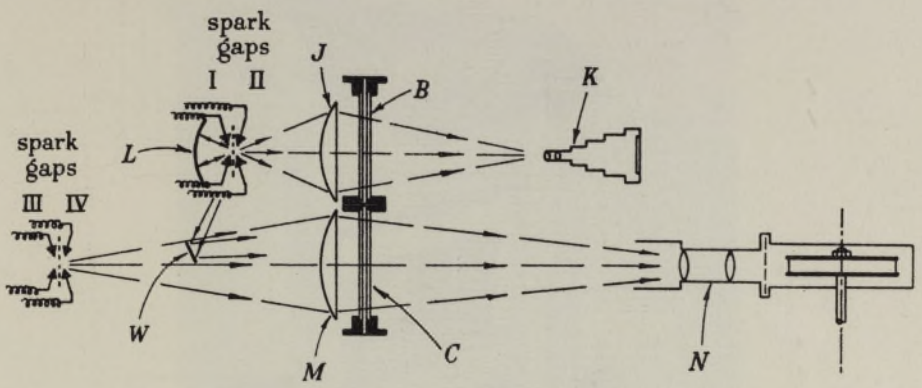

FIGURE 2. The optical system.

The lower window C is illuminated by another pair of spark gaps placed on the optical axis of a condensing lens M which concentrates the beam to pass through the $f/2{\cdot}5$ 7 in. lens N of a rotating drum camera. This lens M covers the whole 9 in. length of the window C.

A photograph of the drum camera is reproduced as figure 3. It consists of an aluminium drum O which carries a length of unperforated 35 mm. film clamped on the outside and can be rotated at speeds up to 7000 r.p.m. by means of the motor P. This motor also drives a shaft carrying a balanced arm Q whose tip passes close to a series of contact screws R mounted on a ring of insulating material. These contact screws are so arranged circumferentially that a set of twenty-four photographs can be spaced evenly around the periphery of the drum O and also that twelve additional photographs can be taken in between the twenty-four previously exposed on the same length of film. The motor P also drives the generator of an electrical speed indicator which gives continuous indication of the motor speed.

The electrical circuits employed to produce the illuminating sparks are shown in figure 4. A valve rectifier is used to provide a source of 5500 V d.c. which is used to charge up a number of separate condensers C_1 and C_3 through high resistances.

The sequence of events making up an experiment are controlled by the pendulum S which is mounted on horizontal pivots and initially in a horizontal position. As it swings downwards it operates a series of switches (not all shown on figure 4) mounted on an arc of insulating material.

Its first action is to make a circuit which energizes two solenoids which open the camera shutters. It then electrically actuates the mechanism to break the glass disk at the bottom of the apparatus approximately 30 msec. later.

Just before the liquid starts to move, the pendulum touches the contact screw T which causes one condenser to discharge across spark gap I which records the initial state of the top surface of the liquid in the plate camera. Soon afterwards the pendulum makes contact with a brass arc U whose length is such that the time of

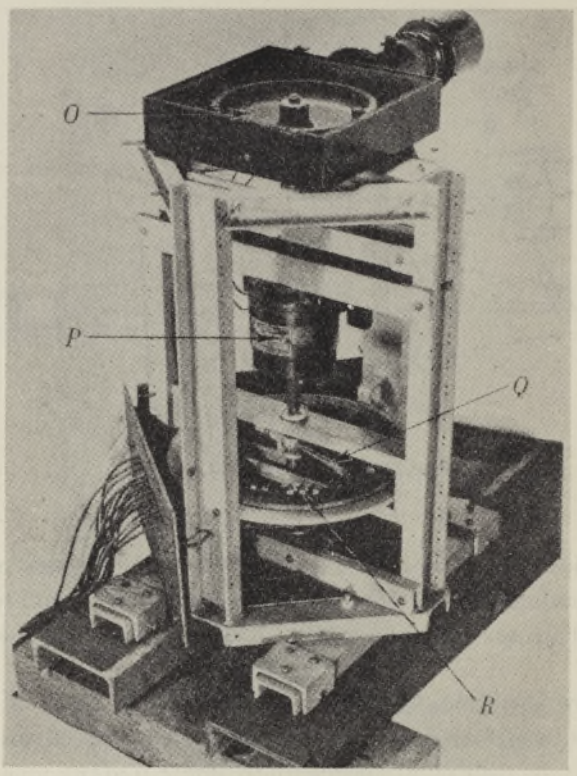

FIGURE 3. The drum camera.

contact is equivalent to one revolution of the drum camera. Whilst contact is made here, twelve condensers discharge across spark gaps II and III in turn when the rotating arm brushes past the appropriate contact screw R. The six sparks across spark gap II record profiles of the downward motion of the top liquid surface on the plate in the plate camera and the other six across spark gap III record the motion of the bottom liquid surface on the length of film.

The succession of up to seven profiles recorded on the stationary plate can be separated easily because the liquid leaves a film on the surface of the windows after the passage of the liquid which interrupts the light beam. The plate on development shows a series of areas of differing densities, the boundaries of which correspond to the top surface profiles.

After this set of photographs, more are taken on the drum camera when the pendulum touches the arc V which allows the rotating arm Q to time twenty-four discharges across spark gap IV. Subsequently, the pendulum causes the camera shutters to be closed and is prevented from swinging back.

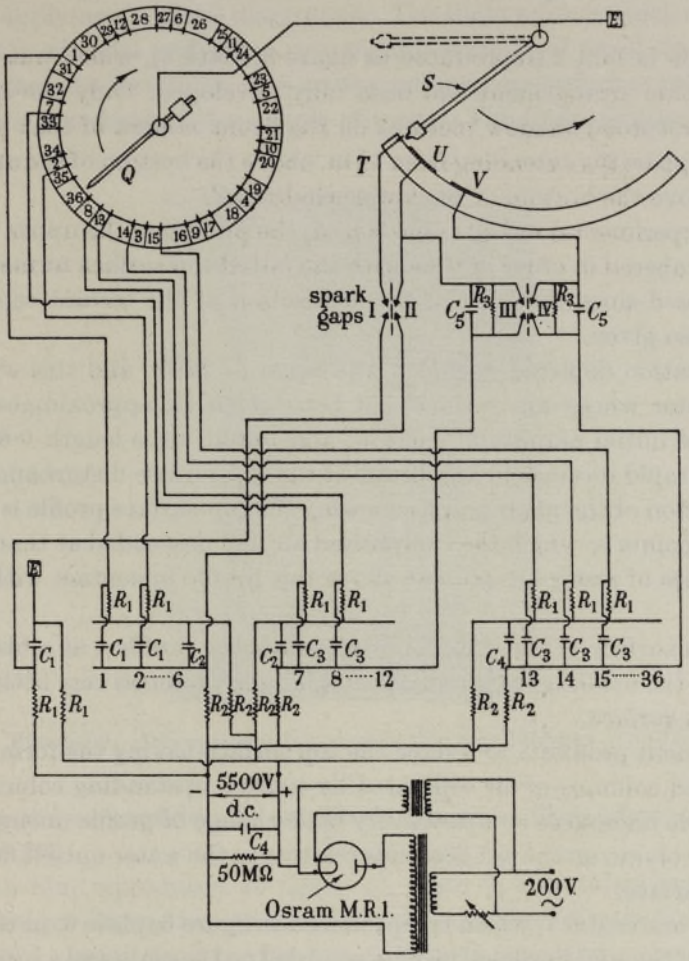

FIGURE 4. The electrical circuits.

$R_1 = 10$ MΩ, $R_2 = 10$ kΩ, $R_3 = 1$ kΩ, $C_1 = 0{\cdot}1\,\mu$F, $C_2 = 0{\cdot}5\,\mu$F, $C_3 = C_5 = 0{\cdot}2\,\mu$F, $C_4 = 1\,\mu$F.

The duration of the discharges across spark gaps III and IV is kept as low as possible by the provision of the condensers C_5 which are situated a few inches from the spark gaps. The spark gaps are 0·030 in. long between pointed copper electrodes.

In order to establish the instant at which each exposure is made in the plate camera, a small beam of light is reflected from spark gaps I and II by the plane mirror W (see figure 2) to illuminate part of the lower pair of windows C.

The plates used in the plate camera were Ilford Ordinary in the majority of experiments, but recourse had to be made to Kodak 0800 plates in a few experiments. The film used in the drum camera was Ilford Recording Film 5G 91.

3. The behaviour of liquid surfaces as recorded experimentally

A considerable number of experiments were made using water as the liquid accelerated under a variety of conditions. Of these, five have been selected for discussion here as being representative of the experiments carried out with water.

The first one is film 2 (reproduced as figure 5, plate 5), which was taken before the photographic arrangement had been fully developed. Only one spark gap was in use which recorded shadow pictures on the drum camera of that portion of the acceleration apparatus extending from 1½ in. above the bottom of the upper windows B to 2½ in. above the bottom of the lower windows C.

In all the experimental records reproduced, the profiles of the upper water surface have been numbered in order of time with the initial top surface termed 0. The time that had elapsed since the start of the accleration at the instant each profile was recorded is also given.

The acceleration depicted in film 2 was equal to $20{\cdot}7g$, and this was applied to 1·14 in. of water whose top surface had been given an approximately sinusoidal disturbance of initial amplitude 0·034 in. and initial wave-length 0·83 in. Profiles 1 to 3 show a rapid increase in amplitude of the top surface disturbance. The top of the white portion of the photographs showing the top-surface profile is the envelope of the lowest points to which the compressed air had descended at that instant, and small quantities of water are present above this profile in contact with the sides of the channel.

The bottom surface of the water is first recorded in profile 4 as a black line. This indicates that the breakage of the shallac diaphragm produces very little disturbance of the bottom surface.

The subsequent profiles 5 to 8 show the top surface having the form of a number of round-ended columns of air separated by narrow upstanding columns of water. The top surface undergoes comparatively little change of profile during this period, whilst the air column on the left descends relative to the water until it finally reaches the bottom surface.

The second one is film 7, which is reproduced as figure 6, plate 6, in the form of an enlargement of the superimposed profiles recorded on the plate and a series of enlargements of the images recorded on the drum camera. Films 28 and 23 are similarly reproduced as figures 7 and 8, plates 7 and 8.

The acceleration depicted in film 7 was equal to $52{\cdot}3g$ acting on 5·29 in. of water, and the initial disturbance was approximately sinusoidal of initial amplitude 0·044 in. and initial wave-length 1·49 in. The increase in amplitude shown in the profiles 1 to 5 is very large. These profiles indicate the envelope of the lowest points to which the compressed air has descended as in the case of film 2, figure 5.

The enlargements from the length of film show considerably less detail in the profile owing to differences in image size and emulsion granularity between the two records. They show that the progressive change from a number of surface troughs and peaks to a smaller number continues until one round-ended column of air remains symmetrically disposed in the acceleration channel.

The characteristics of film 7 are also shown by film 28, figure 7, where 6·80 in. is shown as it was accelerated at 42·8g after being given an initial disturbance of amplitude 0·025 in. and wave-length 0·40 in. The subsequent profiles are in all respects very similar to those shown in film 7 (compare profiles 5 of each film).

Film 23, figure 8, shows what happens when the top liquid surface is accelerated without first applying an initial disturbance. The slight surface tension curvature at the sides of the channel and other unavoidable sources of small disturbances are sufficient to start the instability, but no appreciable top-surface amplitude appears until the water has descended a couple of inches. The later pictures taken on the

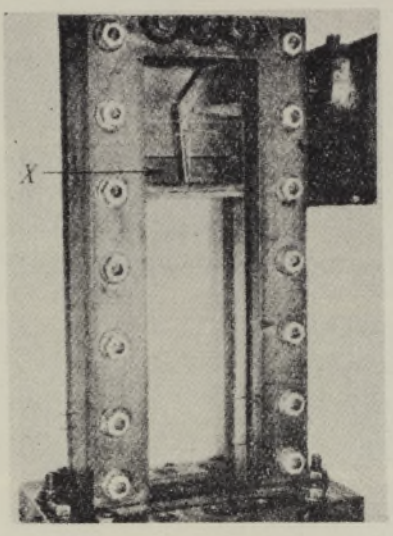

FIGURE 9. Arrangement for accelerating small depths of water.

drum camera show a considerable amplitude similar in all respects to earlier stages of films 7 and 28.

The fourth film reproduced as figure 10, plate 9, was taken using a slightly different technique. It was desired to observe the behaviour of a small depth of water, and to this end a small tank having two thin mica sides and a shellac diaphragm forming its base was inserted between the windows B (see figure 1). The arrangement is shown in figure 9, in which the tank X can be seen containing a small depth of water with the agitating paddle in position to provide the initial surface disturbance. The acceleration apparatus as a whole was lowered so that the windows B were in position for illumination by spark gaps III and IV and recording on the drum camera.

The film 37, figure 10, taken by this method shows the inherent stability of the bottom surface of the water very well. Until the depth of the water (initially 0·62 in.) has been reduced by the steady penetration of the air columns through the water to about $\frac{1}{4}$ in. (profile 4), the bottom surface has remained quite flat. Thereafter it is depressed downwards in front of each air column until the water separating the two volumes of air has been reduced to a thin film. The film of water is then blown out

ahead of the bottom surface (causing the dark areas below it in profile 5) and finally bursts (profile 6).

The behaviour of the top surface shown in film 37 is similar to that observed in films 7 and 28.

The instability as observed experimentally is not two-dimensional owing to the presence of the channel sides and cannot immediately be compared to the theoretical two-dimensional discussion of part I until the magnitude of the deviation from the two-dimension case has been assessed. In order to do this, a small number of experiments were made in which the unstable surface was observed in two vertical planes at right angles.

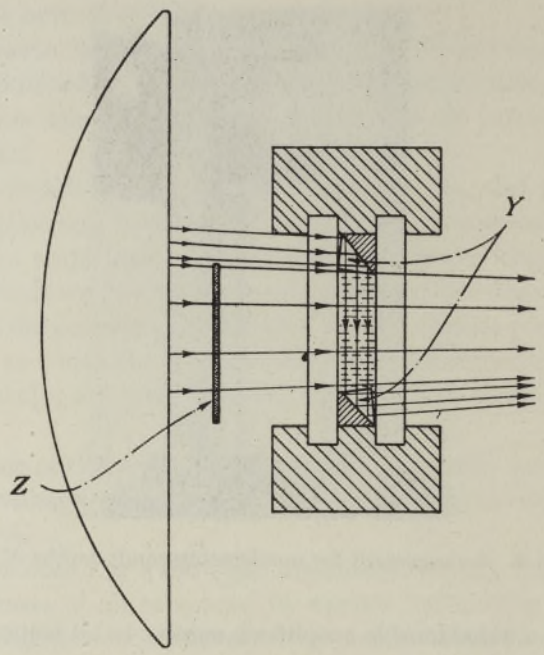

FIGURE 11. Arrangement of cross-viewing prisms.

This was achieved by the use of two prisms inserted in the acceleration channel as shown in the horizontal section reproduced as figure 11. The two prisms Y divert part of the illuminating beam of light to traverse the channel parallel to the faces of the glass windows and then to rejoin the direct beam on its way to the plate camera. A neutral density filter Z was interposed in the direct beam to make the two beams of light of comparable intensity.

The records obtained by the use of this arrangement show that when the top surface has descended about 4 or 5 in. (and has a direct profile of large radius—of the order of 0·5 to 1·0 in.) the cross-profile shown by the prisms had a radius of curvature of 0·225 in. As the half-width of the channel is only 0·250 in., the air column is very nearly in contact with the glass windows and therefore the instability can be regarded as mainly two-dimensional up to this stage.

A few experiments were made to observe the instability of an interface between two non-miscible liquids. One such film is given as figure 12, plate 10, in which

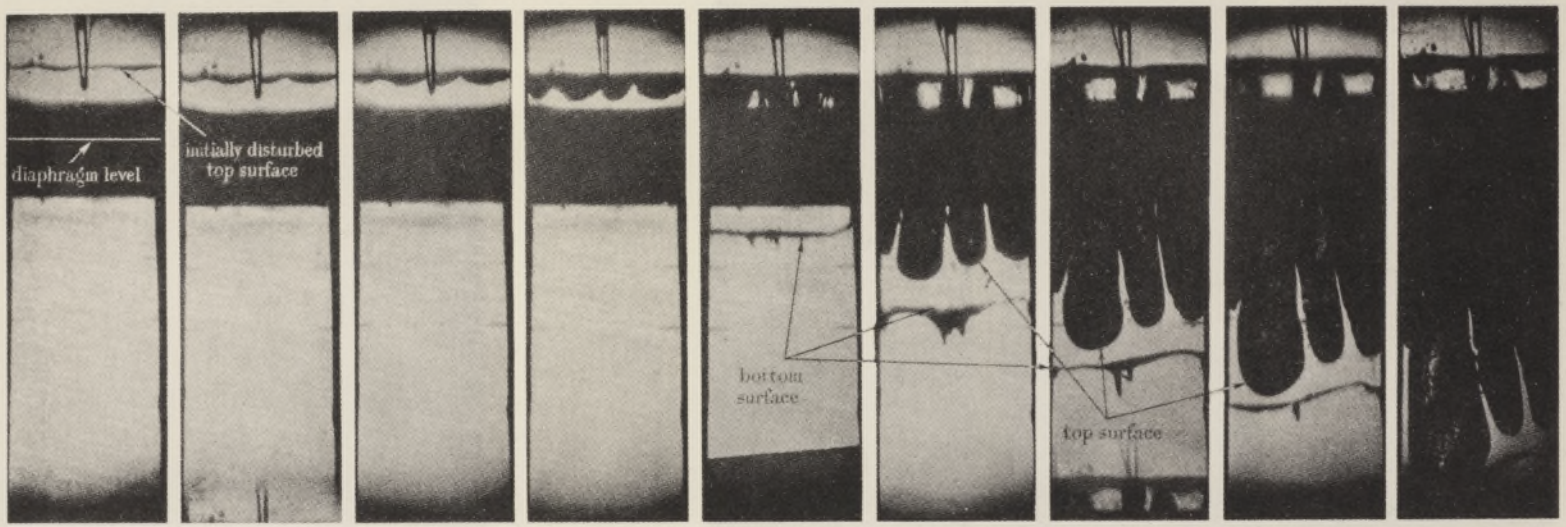

photograph number	0	1	2	3	4	5	6	7	8
time (msec.)		3·39	5·95	8·98	19·25	26·88	31·02	33·35	37·20

FIGURE 5. Acceleration of water; film 2. Depth of water 1·14 in.; initial acceleration = 20·7g.

(*Facing p.* 88)

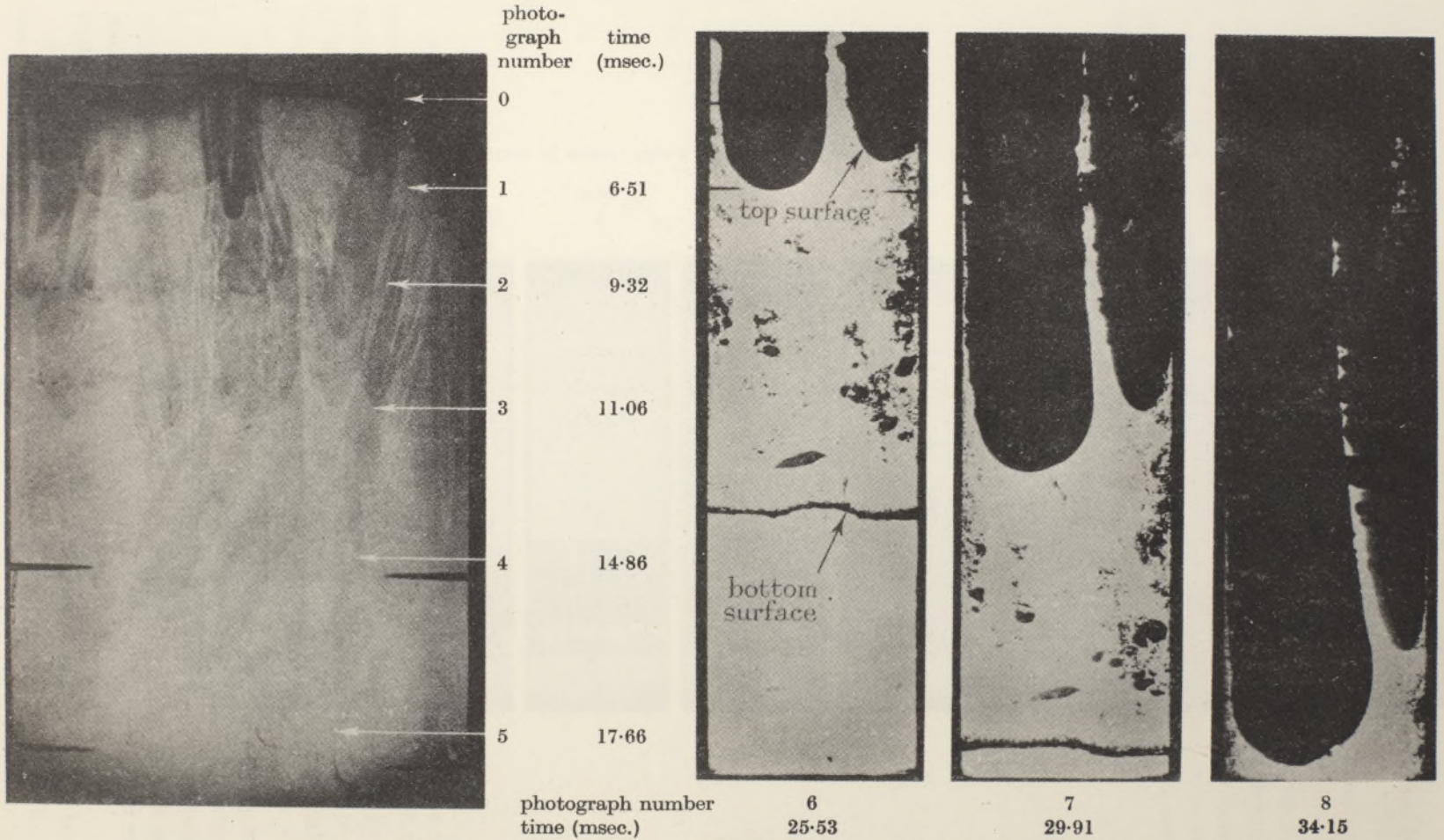

FIGURE 6. Acceleration of water; film 7. Depth of water 5·29 in.; initial acceleration 52·3*g*.

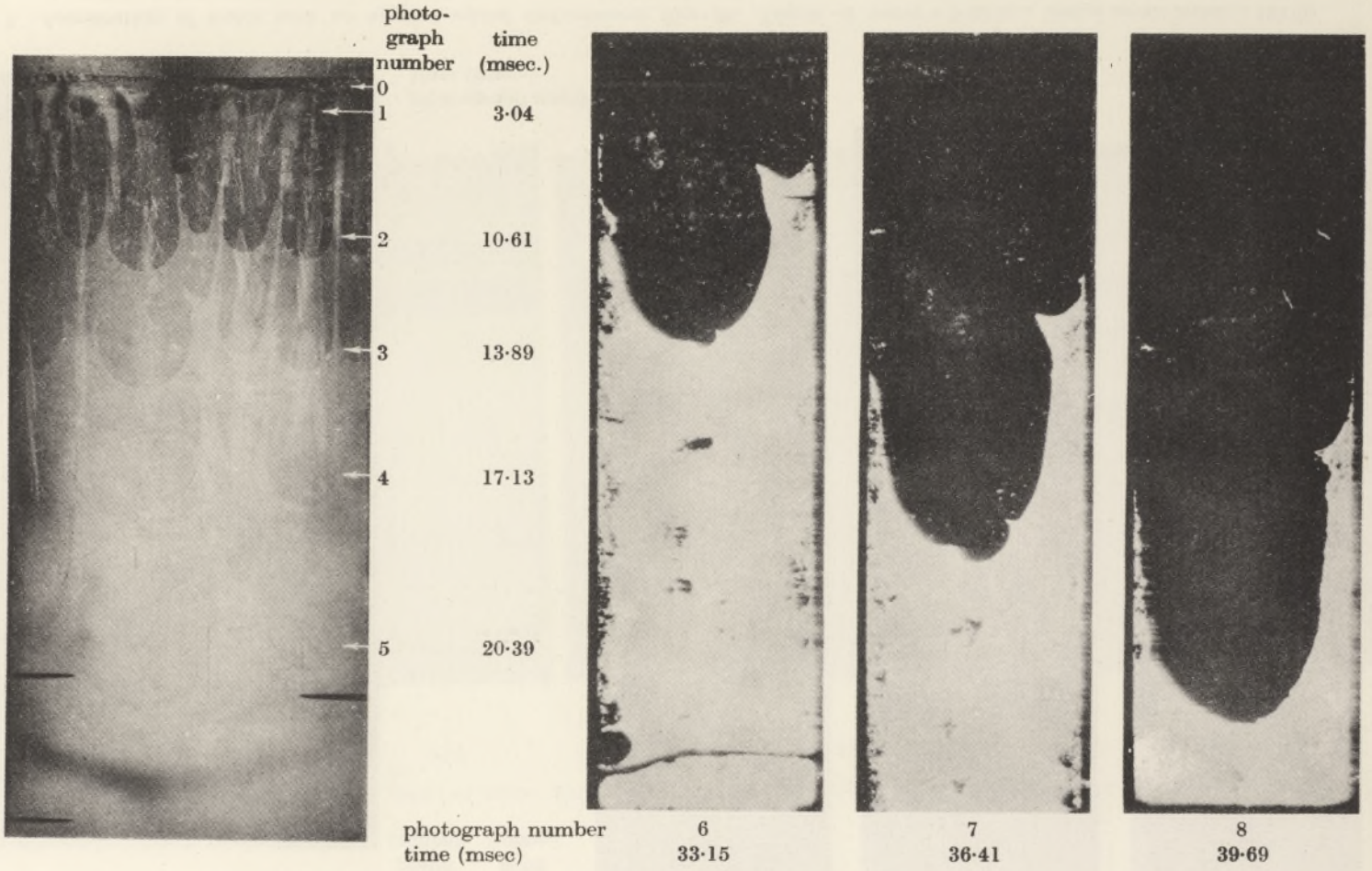

FIGURE 7. Acceleration of water; film 28. Depth of water = 6·80 in.; initial acceleration 42·8*g*.

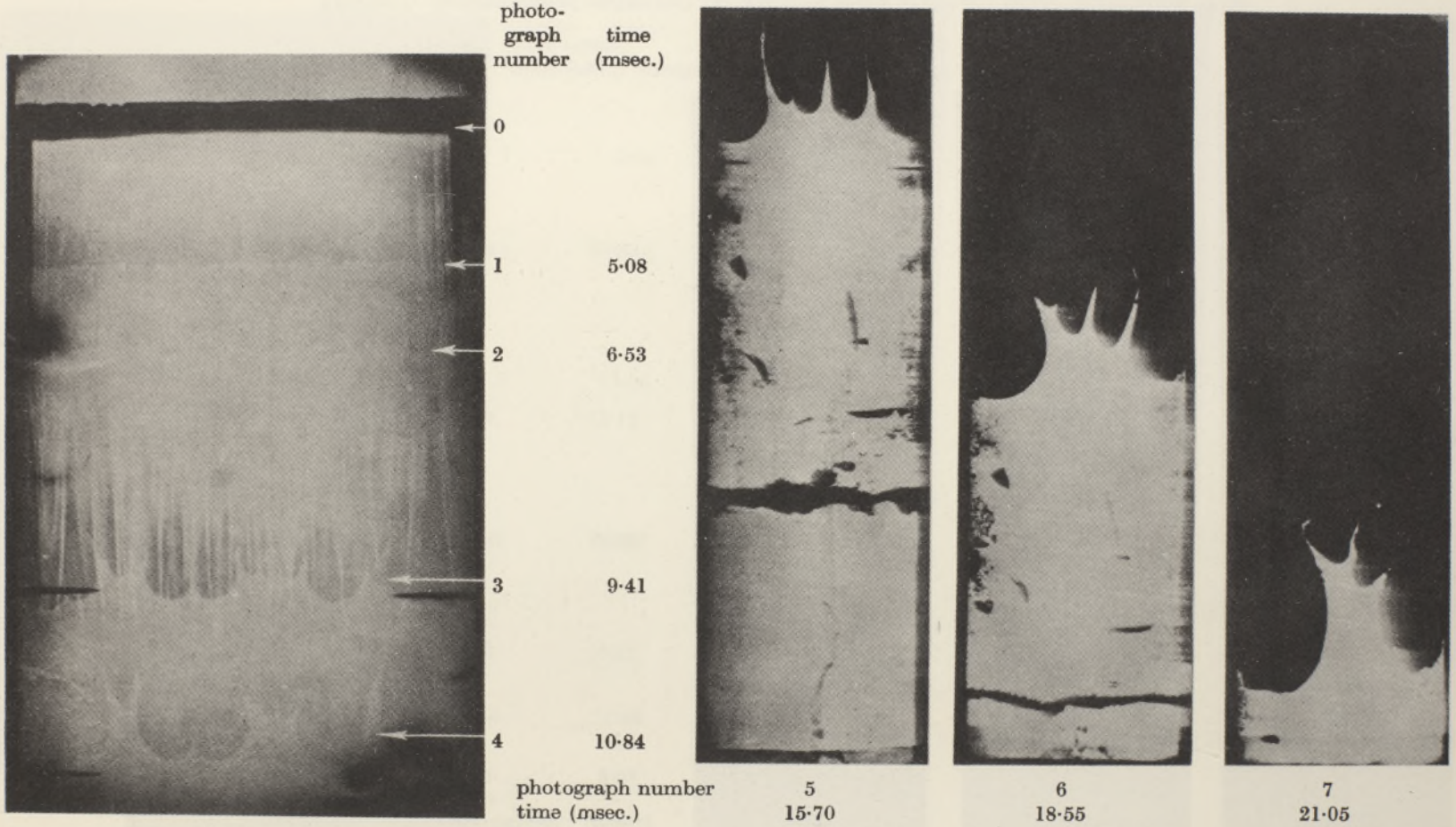

FIGURE 8. Acceleration of water with no applied initial disturbance; film 23. Depth of water = 5·20 in.; initial acceleration = 131·9*g*.

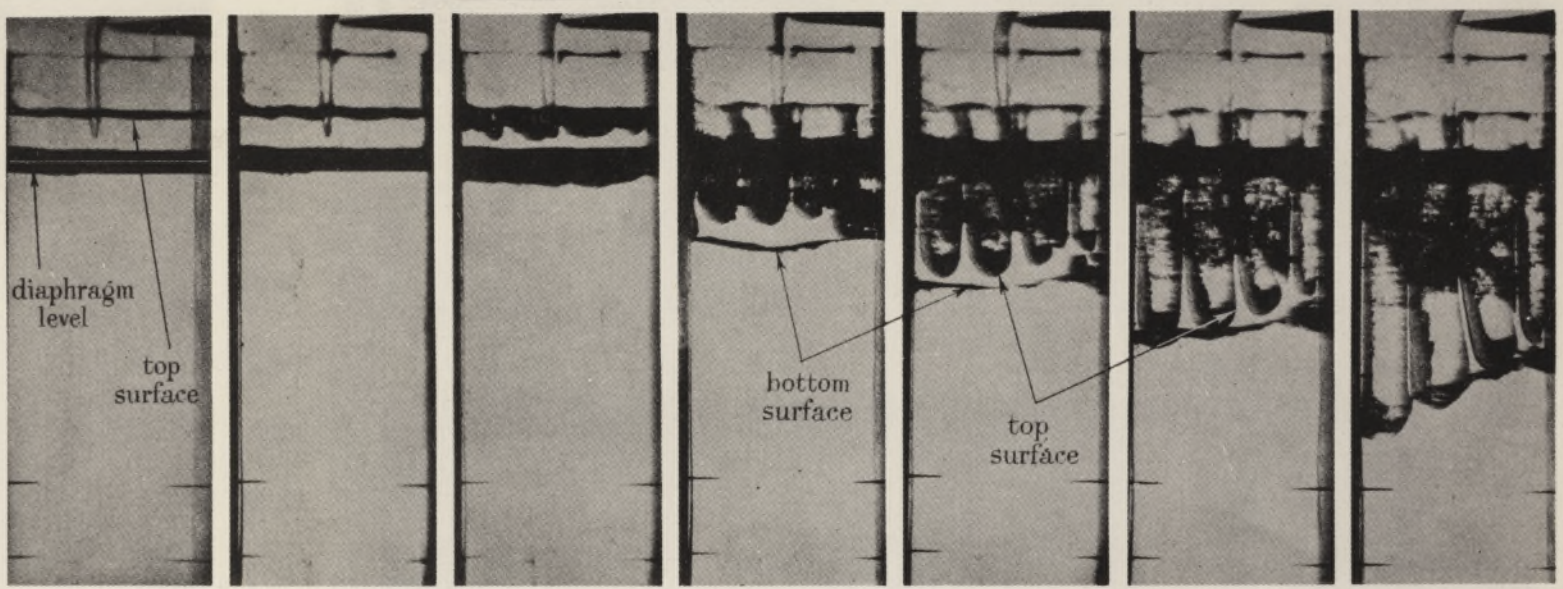

photograph number	0	1	2	3	4	5	6
time (msec.)		3·45	6·06	11·39	13·33	14·63	16·58

FIGURE 10. Acceleration of a small depth of water; film 37. Depth of water = 0·62 in.; initial acceleration = 35·8g.

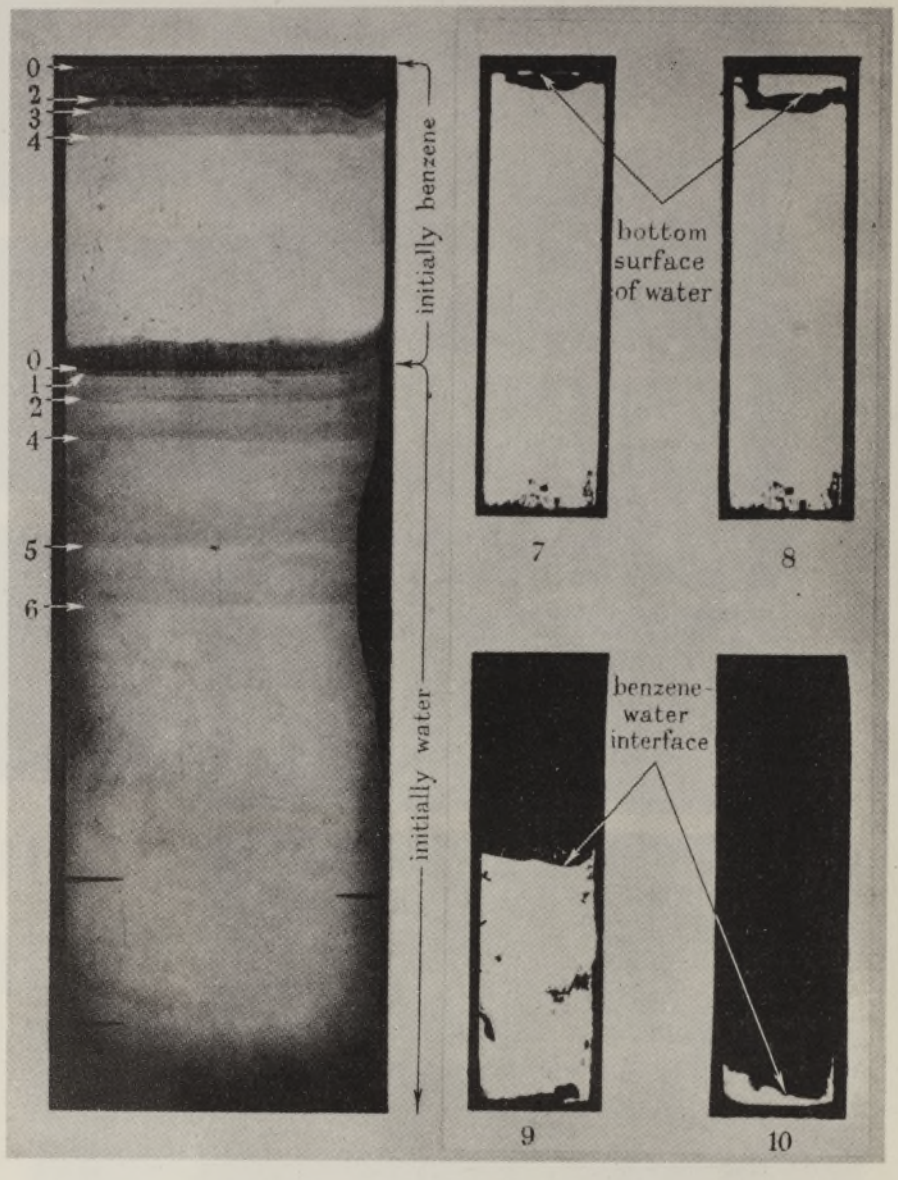

photograph number	1	2	3	4	5	6	7	8	9	10
time (msec.)	5·10	7·57	8·30	10·14	15·21	16·18	12·58	14·62	42·74	49·86

FIGURE 12. Acceleration of benzene-water interface; film 45. Depth of benzene = 2·10 in.; depth of water = 4·70 in.; initial acceleration = 32·1*g*.

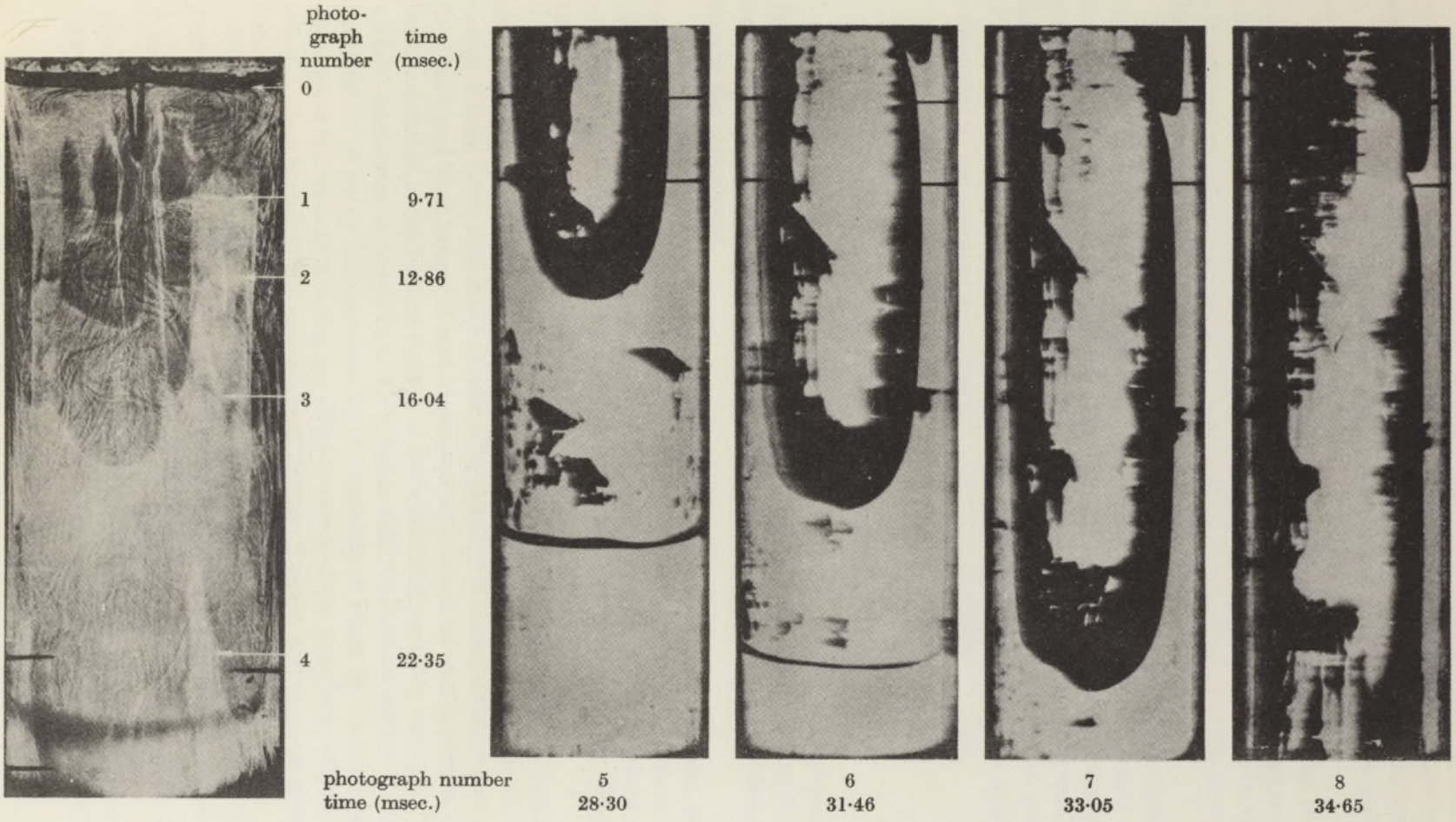

FIGURE 13. Acceleration of glycerine; film 67. Depth of glycerine = 7·88 in.; initial acceleration = 41·4g.

2·10 in. of benzene resting on top of 4·70 in. of water were accelerated at 32·1g. The top surface of the benzene was stabilized by floating a thin strip of balsa wood on it, and an initial slight disturbance given to the interface by means of a pulsating diaphragm placed in the wall of the channel.

The early profiles of the interface (1 to 6) show negligible change, but the two enlargements from the drum camera film (profiles 9 and 10) show that an appreciable amplitude has developed. This decrease in the rate of development of the instability is in full agreement with equation (1), representing the conclusions of the theoretical discussion given in part I.

Finally, a number of experiments were made with glycerine. A representative film is reproduced as figure 13, plate 11. The instability develops in the early stages very similarly to that observed with water, but the later stages differ in that a large quantity of glycerine is left adhering to the sides of the channel, with the result that the air penetrates through the liquid at a much faster rate. Over half of the quantity of glycerine introduced into the apparatus proceeds to drain out of the apparatus subsequent to the actual acceleration and the 10 sec. immediately after.

4. Analysis of the experimental records

The time intervals between successive photographs were established by measuring the distance separating the images or timing marks concerned on the length of film from the drum camera and by reference to the speed of rotation of the drum at the time of the experiment.

The negatives were examined by means of an optical enlarging system, and the mean horizontal levels of the various profiles of the top and bottom surfaces determined. The distances of these horizontal levels from the initial positions of the surfaces were taken as the distances that the top and bottom of the liquid had descended (s_t and s_b respectively).

The acceleration of the liquid was established by plotting $\sqrt{s_t}$ and $\sqrt{s_b}$ against the time intervals. This gave the time of starting of the acceleration from which the values of time t were then made to refer. The plottings of these points are reproduced for films 7 and 23 as figures 14 and 15 respectively. It will be seen in both cases that the acceleration of the bottom surface of the water is remarkably uniform. The top surface accelerates at about 10 to 15 % faster than the bottom surface during the acceleration of water. This is caused by the quantity of water that is left behind on the sides of the channel reducing the effective depth of the main body of water. This effect is accentuated in the case of small depths of water, and is much greater (of the order of 45 %) in the case of glycerine.

With each experiment, the amplitude of the most prominent trough in the disturbance shown in each profile has been measured; and the measurements have been plotted as $\cosh^{-1}\frac{\eta}{\eta_0}$ against $\sqrt{\left\{\frac{s(g_1-g)(\rho_2-\rho_1)}{\lambda g_1(\rho_1+\rho_2)}\right\}}$, using distinctive symbols for the points derived from the various types of experiments. The result is reproduced as figure 16, on which the straight line representing equation (1) is also shown. It is

seen that the points having values of $\sqrt{\left\{\frac{s(g_1-g)(\rho_2-\rho_1)}{\lambda g_1(\rho_1+\rho_2)}\right\}}$ less than about 0·8 are in excellent agreement with equation (1), and that each class of experiment, whether

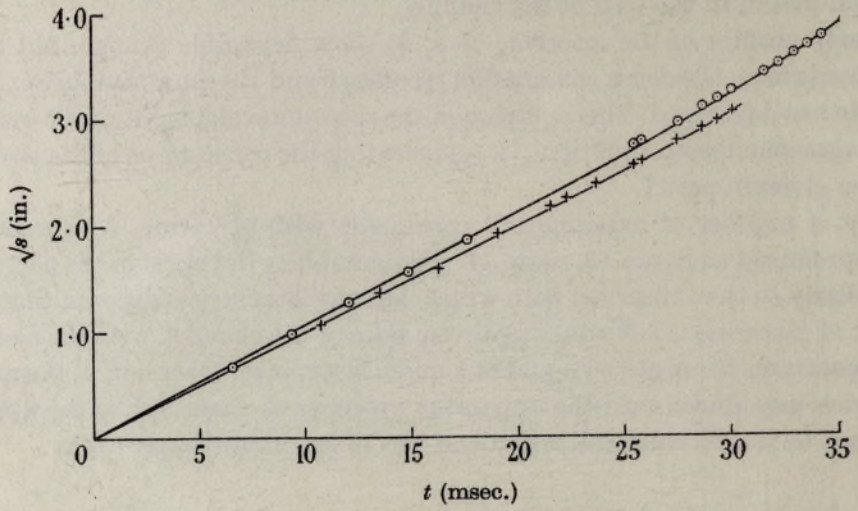

FIGURE 14. $\sqrt{s}$ against t for film 7: ⊙, derived from top surface; +, derived from bottom surface.

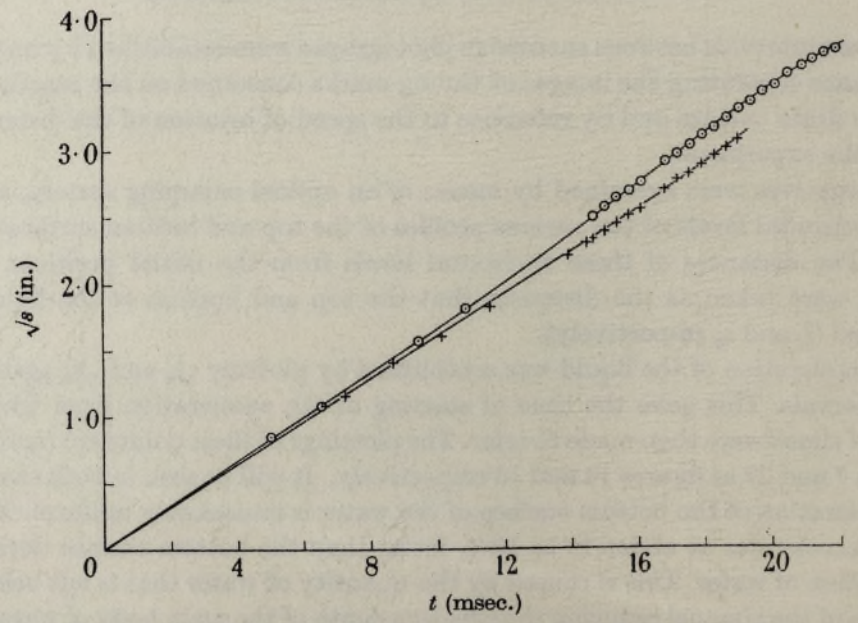

FIGURE 15. $\sqrt{s}$ against t for film 23: ⊙, derived from top surface; +, derived from bottom surface.

dealing with water, glycerine or two liquids, gives rise to points which are scattered throughout the band of experimental points.

To enable further conclusions to be drawn, the points derived from each experiment were plotted and a smooth curve drawn through them. These curves have been combined into two diagrams, figure 17 showing all those derived from liquids of low viscosity and figure 18 showing those derived from the experiments with glycerine.

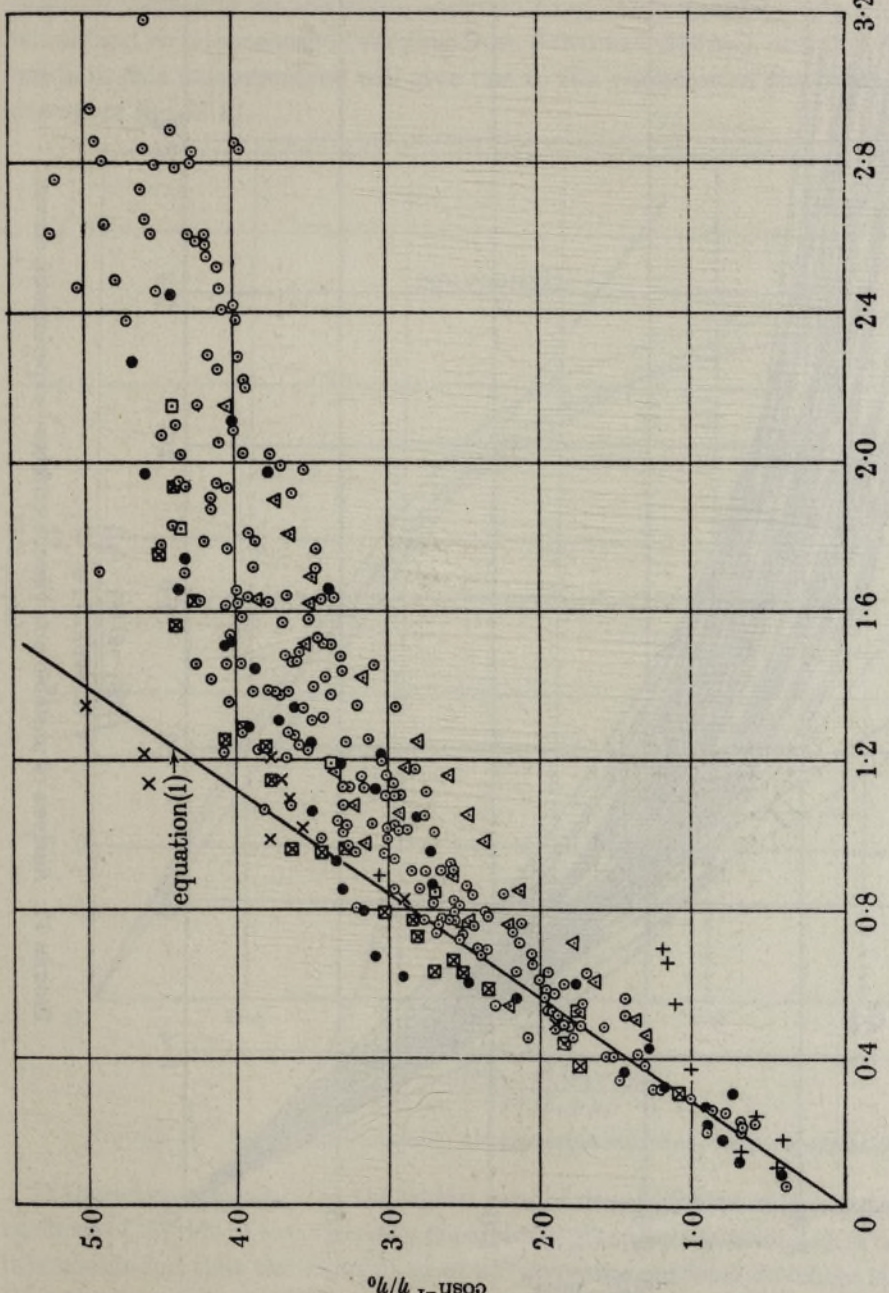

FIGURE 16. Analysis of unstable surfaces—experimental points: ⊙, $g_1 > 10g$ and $h > 1{\cdot}5$ in.; △, $g_1 < 10g$ and $h > 1{\cdot}5$ in.; ●, $h < 1{\cdot}5$ in.; air-water surfaces: ⊡, air-benzene surfaces; ×, water-carbon tetrachloride surfaces; +, benzene-water surfaces; ×, air-glycerine surfaces.

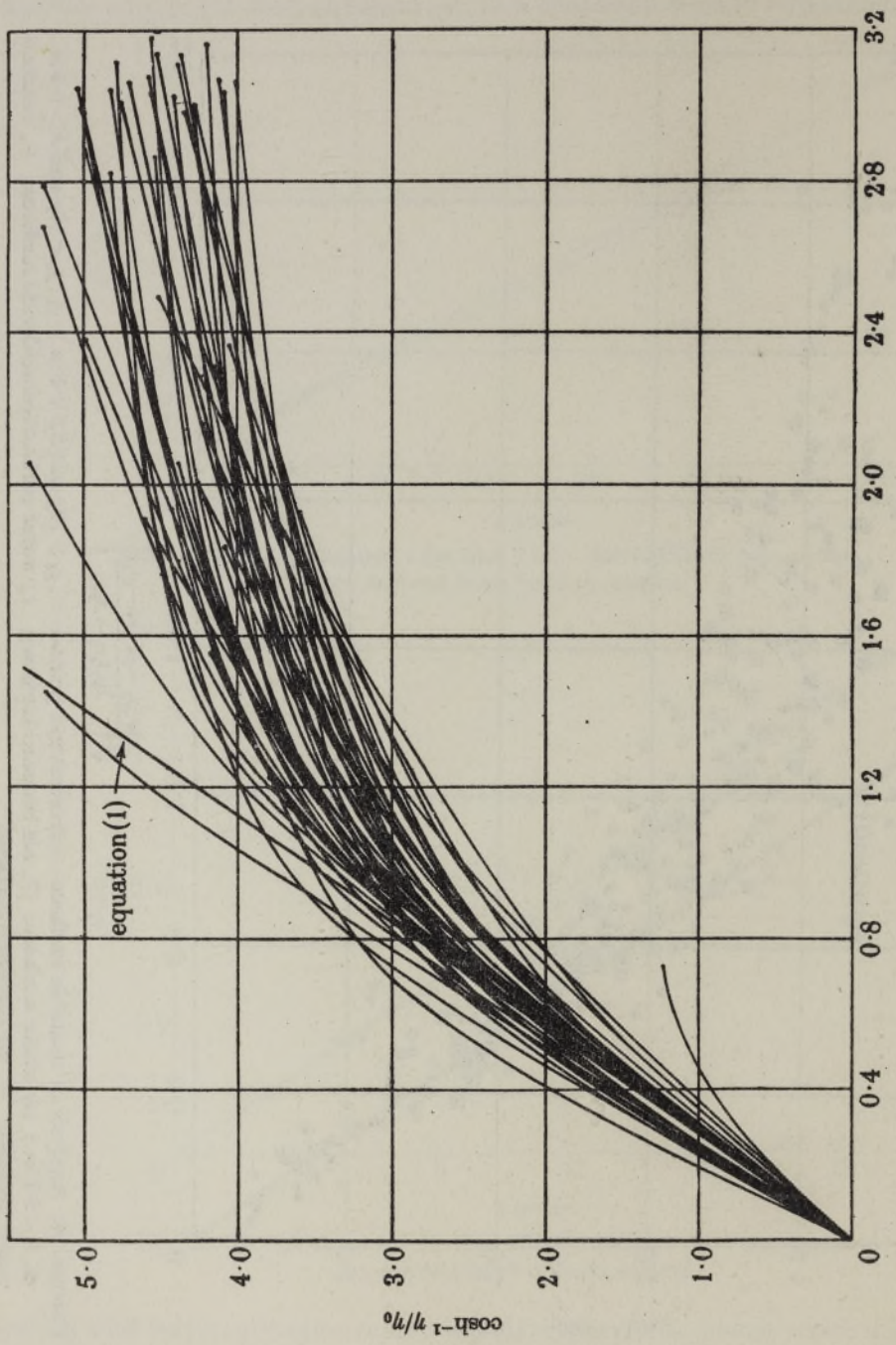

FIGURE 17. Analysis of unstable non-viscous surfaces—experimental curves.

The initial slopes of the curves shown in figure 17 show a considerable variation, but are equally distributed on either side of the line corresponding to equation (1).

The experimental points through which these curves were drawn depend for their position vertically on the value assigned to η_0. This quantity was the smallest one which had to be measured (varying from 0·005 to 0·336 in.), and unavoidable errors made in this measurement will give rise to the variation of the initial slopes of the curves of figure 17.

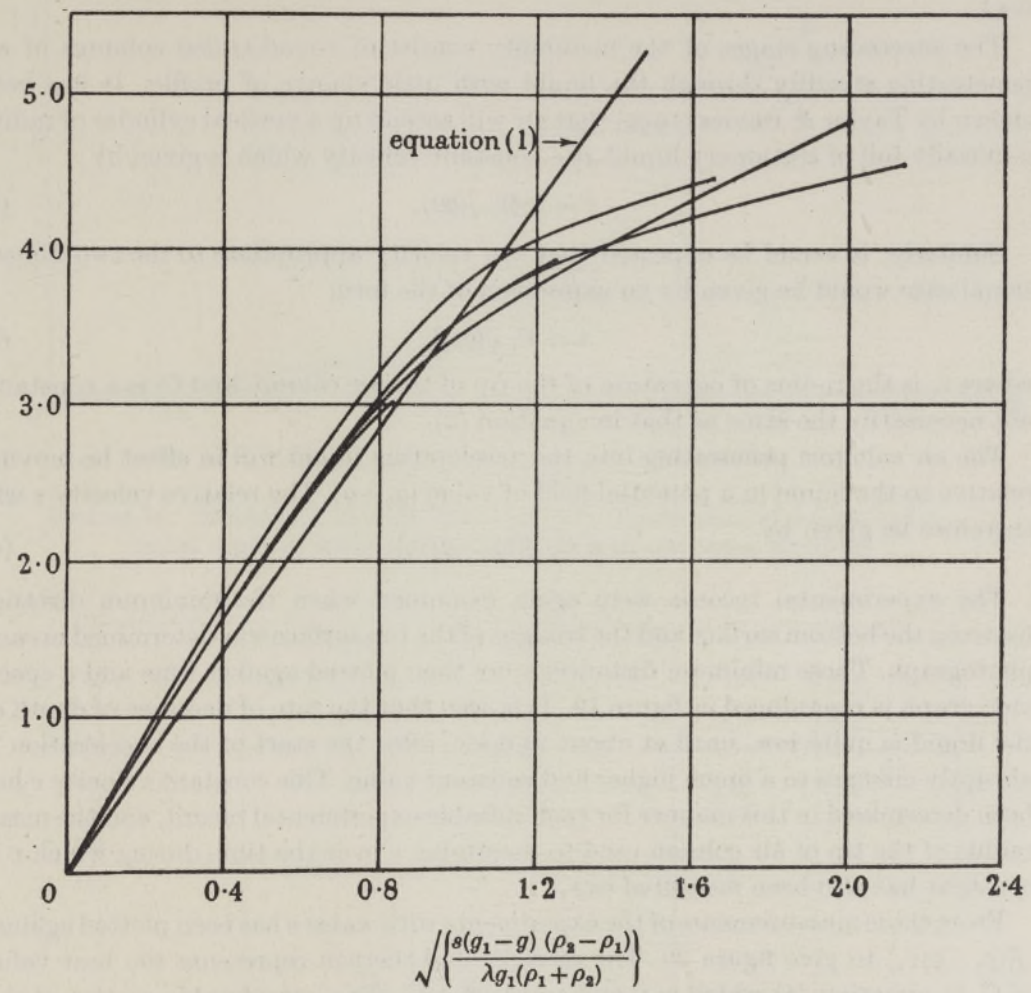

FIGURE 18. Analysis of unstable air-glycerine surfaces—experimental curves.

It therefore appears that the initial rate of development of the instability of the surfaces of liquids of low viscosity is correctly given by equation (1). From figure 18, it is concluded that the instability of air-glycerine surfaces develops slightly faster than that given by equation (1), but this is probably due to the viscous drag exerted by the channel sides and would be much reduced in the case of a channel of larger cross-section.

The point on each curve at which the slope is equal to half that of the line representing equation (1) has been determined, and the ratio of η_{c_1} (the amplitude at this point) to λ has been calculated. This ratio η_{c_1}/λ represents the shape of the unstable

disturbance at the time when it is ceasing to increase at the rate given by the first-order theory.

The values of η_{c_1}/λ range from 0·11 to 0·96 with 75 % of them between 0·23 and 0·63. As these values will be dependent on the positions of the experimental points of figure 16 (which are determined by the estimation of the value of η_0 as explained above), it seems that these results may be interpreted roughly as showing that the instability follows the first-order theory until it has attained an amplitude of about $0{\cdot}4\lambda$.

The succeeding stages of the instability consist of round-ended columns of air penetrating steadily through the liquid with little change of profile. It has been shown by Taylor & Davies (1950) that air will ascend up a vertical cylinder of radius a initially full of stationary liquid at a constant velocity which is given by

$$v = 0{\cdot}48\sqrt{(ga)}. \tag{2}$$

Similarly, it would be expected that the velocity appropriate to the two-dimensional case would be given by an expression of the form

$$v = C_1\sqrt{(gr_1)}, \tag{3}$$

where r_1 is the radius of curvature of the tip of the air column and C_1 is a constant, not necessarily the same as that in equation (2).

The air columns penetrating into the accelerating liquid will in effect be moving relative to the liquid in a potential field of value (g_1-g). The relative velocity v will therefore be given by

$$v = C_1\sqrt{\{(g_1-g)r_1\}}. \tag{4}$$

The experimental records were again examined when the minimum distance between the bottom surface and the troughs of the top surface was determined in each photograph. These minimum distances were then plotted against time and a specimen graph is reproduced as figure 19. It is seen that the rate of decrease of depth of the liquid is quite low, until at about $9\frac{1}{2}$ msec. after the start of the acceleration it abruptly changes to a much higher and constant value. This constant velocity v has been determined in this manner for each suitable experimental record, and the mean radius of the tip of air column used to determine v over the time during which v is constant has also been measured as r_1.

From these measurements of the experiments with water v has been plotted against $\sqrt{\{(g_1-g)r_1\}}$ to give figure 20. The straight line thereon represents the best value of C_1 in equation (4) which is found to equal 1·11. The considerable scatter of the points is partly due to errors arising in the measurement of r_1 and partly due to the assumption that the experiments are truly two-dimensional. It has been shown that the velocity is accurately proportional to $\sqrt{(g_1-g)}$ but not to $\sqrt{r_1}$. Equation (4) with $C_1 = 1{\cdot}11$ over-estimates the value of v when r_1 is small (about 0·25 in.) and underestimates the value of v when r_1 is large (about 0·9 in.).

Similar measurements of air-glycerine surfaces give very much higher values of v, which require the value of C_1 to be between 3·5 and 5·5 (according to the value of the viscosity) for equation (4) to predict the measured values of v. This increase in the penetration velocity is due to the influence of the sides of the channel and would not be observed in channels of larger section.

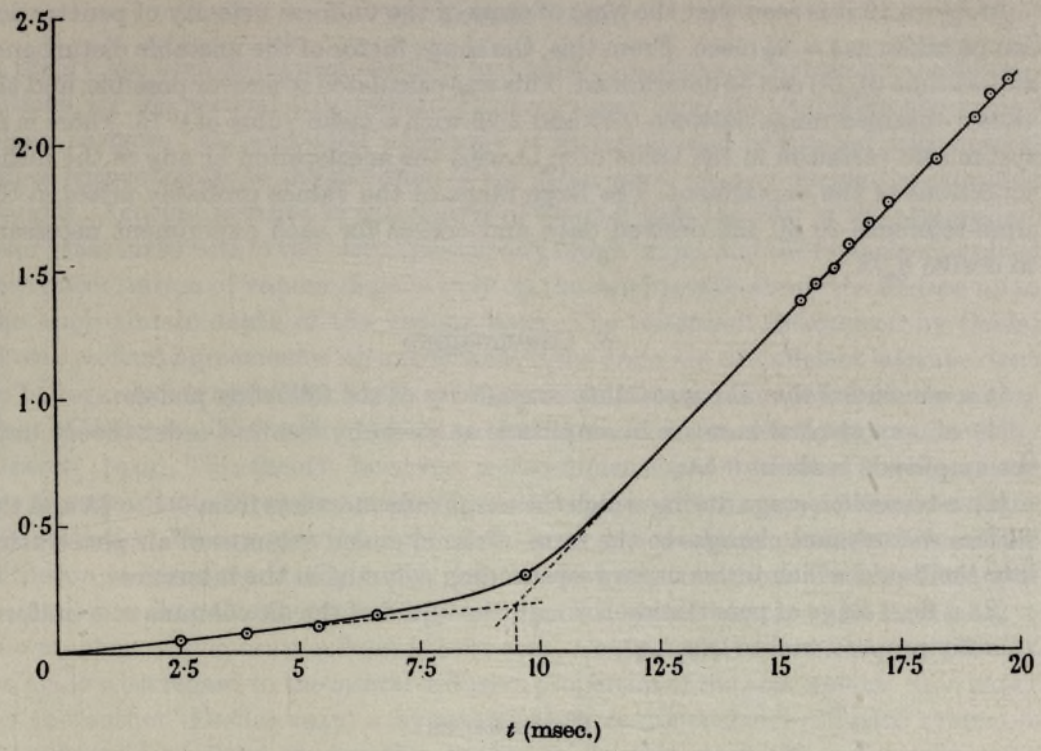

FIGURE 19. Penetration of water by air column. Acceleration of water = 118·5g; initial depth of water = 5·01 in.; radius of tip of column = 0·80 in.

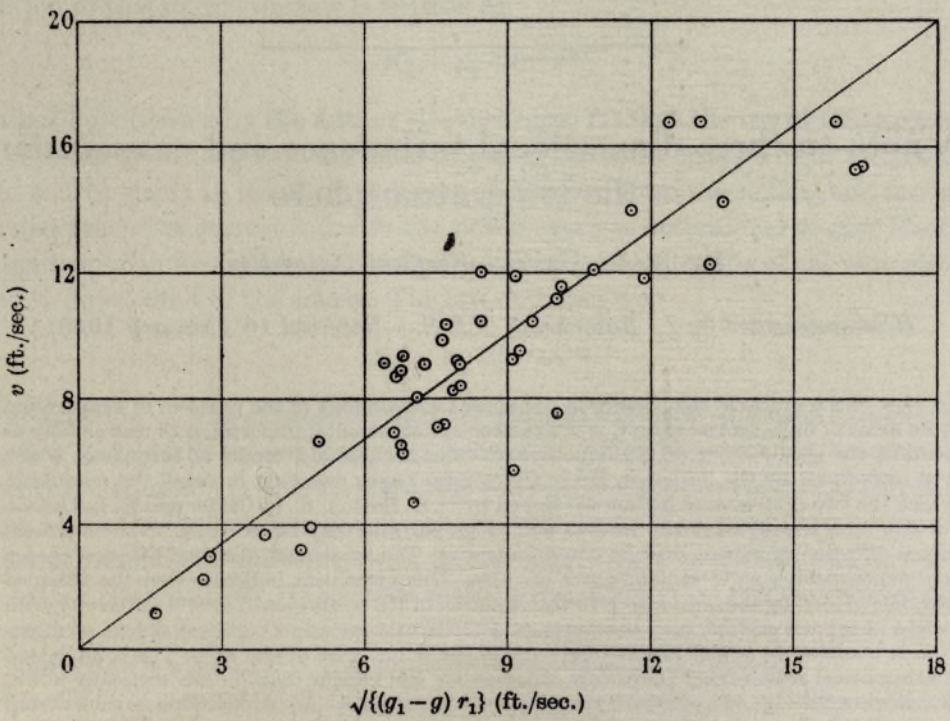

FIGURE 20. Penetration velocities compared with equation (4), $v = 1{\cdot}11\sqrt{\{(g_1 - g)\, r_1\}}$.

In figure 19 it is seen that the time of start of the uniform velocity of penetration can be taken as $t = 9\frac{1}{2}$ msec. From this, the shape factor of the unstable disturbance at that time (η_{c_2}/λ) can be determined. This was calculated wherever possible, and the values obtained range between 0·05 and 2·26 with a mean value of 0·75. There is no systematic variation in the value of η_{c_2}/λ with the acceleration or any of the initial conditions of the experiment. The large range of the values probably arises in the cross-reference to all the derived data and curves for each experiment necessary to derive η_{c_2}/λ.

5. Conclusions

It is concluded that the instability is made up of the following phases:

(1) an exponential increase in amplitude as given by the first-order theory until the amplitude is about $0{\cdot}4\lambda$;

(2) a transition stage during which the amplitude increases from 0·4 to $\frac{3}{4}\lambda$ and the surface disturbance changes to the form of round-ended columns of air penetrating into the liquid which forms narrow upstanding columns in the interstices;

(3) a final stage of penetration through the liquid of the air columns at a uniform velocity proportional to $\sqrt{(g_1 - g)}$.

References

Davies, R. M. & Taylor, Sir. G. 1950 *Proc. Roy. Soc.* A, **200**, 375.
Taylor, Sir G. 1950 *Proc. Roy. Soc.* A, **201**, 192 (Part I).

A note on three-dimensional turbulence and evaporation in the lower atmosphere

By D. R. Davies, *Sheffield University*

(*Communicated by L. Rosenhead, F.R.S.—Received* 10 *January* 1950)

In view of the practical significance in dynamical meteorology of the problem of evaporation from areas of finite lateral extent, it is a matter of fundamental importance to test as fully as possible the applicability of the hypothetical three-dimensional model of turbulence which was introduced by the author in 1947. The present paper describes in detail the manner in which the two-dimensional system developed by O. G. Sutton, K. L. Calder and E. L. Deacon for flow over aerodynamically smooth and rough surfaces may be extended to three-dimensional diffusion of vapour over an *evaporating* area. The agreement obtained between theory and experiment is good at points *over* the area. This agreement indicates that the assumed law, introduced by the author to give the variation of the coefficient of lateral diffusivity with height above the surface, may be used satisfactorily in *evaporation* problems as long as attention is confined to points not too far outside the boundaries of the area. The complicated mathematical relationship previously obtained for the vapour distribution vertically above the down-wind edge of a parabolic strip is reduced to a much simpler one. This serves to bring out explicitly the relationship between the effects of the two- and three-dimensional theoretical systems of turbulent transfer at points on the central axis of the area.